

# Cannabinoid 1 Receptor Promotes Cardiac Dysfunction, Oxidative Stress, Inflammation, and Fibrosis in Diabetic Cardiomyopathy

Mohanraj Rajesh,<sup>1</sup> Sándor Bátkai,<sup>1,2</sup> Malek Kechrid,<sup>1</sup> Partha Mukhopadhyay,<sup>1</sup> Wen-Shin Lee,<sup>1</sup> Béla Horváth,<sup>1</sup> Eileen Holovac,<sup>1</sup> Resat Cinar,<sup>1</sup> Lucas Liaudet,<sup>3</sup> Ken Mackie,<sup>4</sup> György Haskó,<sup>5</sup> and Pál Pacher<sup>1</sup>

Endocannabinoids and cannabinoid 1 (CB<sub>1</sub>) receptors have been implicated in cardiac dysfunction, inflammation, and cell death associated with various forms of shock, heart failure, and atherosclerosis, in addition to their recognized role in the development of various cardiovascular risk factors in obesity/metabolic syndrome and diabetes. In this study, we explored the role of CB<sub>1</sub> receptors in myocardial dysfunction, inflammation, oxidative/nitrative stress, cell death, and interrelated signaling pathways, using a mouse model of type 1 diabetic cardiomyopathy. Diabetic cardiomyopathy was characterized by increased myocardial endocannabinoid anandamide levels, oxidative/nitrative stress, activation of p38/Jun NH<sub>2</sub>-terminal kinase (JNK) mitogen-activated protein kinases (MAPKs), enhanced inflammation (tumor necrosis factor- $\alpha$ , interleukin-1 $\beta$ , cyclooxygenase 2, intracellular adhesion molecule 1, and vascular cell adhesion molecule 1), increased expression of CB<sub>1</sub>, advanced glycation end product (AGE) and angiotensin II type 1 receptors (receptor for advanced glycation end product [RAGE], angiotensin II receptor type 1 [AT<sub>1</sub>R]), p47(phox) NADPH oxidase subunit,  $\beta$ -myosin heavy chain isozyme switch, accumulation of AGE, fibrosis, and decreased expression of sarcoplasmic/endoplasmic reticulum Ca<sup>2+</sup>-ATPase (SERCA2a). Pharmacological inhibition or genetic deletion of CB<sub>1</sub> receptors attenuated the diabetes-induced cardiac dysfunction and the above-mentioned pathological alterations. Activation of CB<sub>1</sub> receptors by endocannabinoids may play an important role in the pathogenesis of diabetic cardiomyopathy by facilitating MAPK activation, AT<sub>1</sub>R expression/signaling, AGE accumulation, oxidative/nitrative stress, inflammation, and fibrosis. Conversely, CB<sub>1</sub> receptor inhibition may be beneficial in the treatment of diabetic cardiovascular complications. *Diabetes* 61:716–727, 2012

**I**n diabetic patients, cardiovascular complications represent the principal cause of morbidity and mortality. Myocardial left ventricular (LV) dysfunction (both diastolic and later systolic) independent of

atherosclerosis and coronary artery disease has been well documented in both humans and animals (1,2). The mechanisms of diabetic cardiomyopathy are multifaceted, involving increased oxidative/nitrosative stress (3–6), accumulation of advanced glycation end products (AGEs) (7–9), enhanced receptor for advanced glycation end product (RAGE) and angiotensin II receptor type 1 (AT<sub>1</sub>R) signaling (3,7–13), activation of various proinflammatory and cell death signaling pathways [e.g., poly(ADP-ribose) polymerase (PARP)], mitogen-activated protein kinases (MAPKs) (10,14–16), coupled with consequent changes in the composition of extracellular matrix with enhanced cardiac fibrosis (13,16), myosin heavy chain (MHC) isoform switch (17), and decreased activity of sarcoplasmic/endoplasmic reticulum Ca<sup>2+</sup>-ATPase (SERCA2a) (18–20), just to mention a few.

Recent preclinical and clinical studies have importantly implicated endocannabinoids (novel lipid mediators) and cannabinoid 1 (CB<sub>1</sub>) receptors (CB<sub>1</sub>Rs) in the regulation of food intake, energy balance, and metabolism (21–23). CB<sub>1</sub>R inhibition with rimonabant (SR141716/SR1) demonstrated multiple beneficial effects on metabolic and inflammatory markers both in obese and/or type 2 diabetic patients, as well as in various preclinical disease models (21,23). CB<sub>1</sub>Rs are predominantly expressed in the central nervous system (21), but are also present in cardiovascular and virtually all other peripheral tissues, albeit at much lower levels (24,25). In the cardiovascular system, CB<sub>1</sub> activation by endocannabinoids or synthetic ligands leads to complex cardiovascular depressive effects, implicated in the cardiovascular collapse associated with various forms of shock (21) and heart failure (26–28). CB<sub>1</sub>R activation in coronary artery endothelial cells (29), cardiomyocytes (26,27), and inflammatory cells (28,30) mediates MAPK activation, reactive oxygen species (ROS) generation, and inflammatory response promoting atherosclerosis (31) and cardiac dysfunction (27,28). Furthermore, elevated endocannabinoid plasma levels have recently been associated with coronary circulatory dysfunction in human obesity (32), and CB<sub>1</sub>R blockade or its genetic deletion attenuated proteinuria and/or vascular inflammation and cell death in experimental models of type 1 diabetic nephropathy (33) and/or retinopathy (34). Beneficial effect of CB<sub>1</sub> blockade has also been reported in rodent models of type 1 diabetic neuropathy and in various high glucose-induced in vitro experimental paradigms (rev. in 35).

In this study, we investigated the potential role of the endocannabinoids and CB<sub>1</sub>R in the pathogenesis of type 1 diabetic cardiomyopathy using selective CB<sub>1</sub>R inhibitors or CB<sub>1</sub> knockout mice. Our results demonstrate that pharmacological inhibition or genetic deletion of CB<sub>1</sub> attenuates

From the <sup>1</sup>Laboratory of Physiological Studies, National Institutes of Health, National Institute on Alcohol Abuse and Alcoholism, Bethesda, Maryland; the <sup>2</sup>Institute for Molecular and Translational Therapeutic Strategies, Hannover Medical School, Hannover, Germany; the <sup>3</sup>Department of Intensive Care Medicine, University Hospital, Lausanne, Switzerland; the <sup>4</sup>Department of Psychological and Brain Sciences, Indiana University, Bloomington, Indiana; and the <sup>5</sup>Department of Surgery, University of Medicine and Dentistry of New Jersey–New Jersey Medical School, Newark, New Jersey.

Corresponding author: Pál Pacher, pacher@mail.nih.gov.  
Received 8 April 2011 and accepted 6 December 2011.

DOI: 10.2337/db11-0477

This article contains Supplementary Data online at <http://diabetes.diabetesjournals.org/lookup/suppl/doi:10.2337/db11-0477/-/DC1>.

M.R. and S.B. contributed equally to this work.

© 2012 by the American Diabetes Association. Readers may use this article as long as the work is properly cited, the use is educational and not for profit, and the work is not altered. See <http://creativecommons.org/licenses/by-nc-nd/3.0/> for details.

cardiac dysfunction, oxidative stress, inflammation, and fibrosis in diabetic mice.

## RESEARCH DESIGN AND METHODS

**Animals and treatment.** Animal protocols used in this study adhered to the National Institutes of Health (NIH) guidelines and were approved by the Institutional Animal Care and Use Committee of the National Institute on Alcohol Abuse and Alcoholism (NIAAA). Diabetes was induced in 8- to 12-week-old C57/BL6J(WT) mice (male, The Jackson Laboratories, Bar Harbor, ME) or  $CB_1^{+/+}$   $CB_1^{-/-}$  mice (on C57/BL6J background; Intramural Research Program of NIH/NIAAA, Rockville, MD) weighing 23–25 g by intraperitoneal administration of streptozotocin (STZ) (Sigma, St. Louis, MO) at the dose of 50 mg/kg dissolved in 100 mmol/L citrate buffer, pH 4.5, for 5 consecutive days as described (16). After 5 days, the blood glucose levels were measured using an Ascensia Counter Glucometer (Bayer HealthCare, Tarrytown, NY) by mandibular puncture blood sampling. Only mice that had blood glucose values  $>250$  mg/dL were used for the study. Control animals were administered the same volume of citrate buffer, and all mice had access to food and water ad libitum. Diabetes was allowed to develop further for 1 additional week before animals were treated for 11 weeks with the selective  $CB_1R$  antagonists (SR141716A/rimonabant and AM281; 10 mg/kg i.p. daily; National Institute on Drug Abuse Drug Supply Program, Research Triangle Park, NC) or corresponding vehicle. After 12 weeks, animals were subjected to hemodynamic measurements (described below), and hearts were excised and snap-frozen in liquid nitrogen for biochemical determinations or fixed in formalin for histological evaluations. The treatment protocols are detailed in Supplementary Figs. 1 and 2. In a separate set of experiments, 8-week diabetic mice were treated with SR141716A/rimonabant or vehicle for 4 weeks before hemodynamic measurements (Supplementary Fig. 6).

**Hemodynamic measurements.** LV performance was measured and evaluated in mice anesthetized with 2% isoflurane using a 1F microtip pressure-volume catheter (PVR 1045; Millar Instruments, Houston, TX) coupled with an ARIA pressure-volume conductance system (Millar Instruments) and a Powerlab/4SP A/D converter (AD Instruments, Mountain View, CA), as previously described (26,36).

**Determination of myocardial endocannabinoids content.** Hearts were excised and immediately snap-frozen in liquid nitrogen, and samples were stored in  $-80^\circ\text{C}$  until analysis. Endocannabinoids anandamide (*N*-arachidonylethanolamide; AEA) and *N*-arachidonyl-glycerol (2-AG) in various heart tissues were determined with liquid chromatography–mass spectrophotometry as previously described (26).

**Pancreas insulin content.** Pancreatic insulin content was determined using the kit obtained from ALPCO Diagnostics (Salem, NH), by following the extraction procedure described previously (16).

**Determination of HbA<sub>1c</sub>.** HbA<sub>1c</sub> levels in EDTA whole blood was determined using the commercially available reagents procured from Stanbio Laboratory (Boerne, TX) (16).

**Reverse transcription and real-time PCR.** LV myocardial tissues were homogenized and total RNA was isolated using TRIzol reagent (Invitrogen, Carlsbad, CA) according to the manufacturer's instruction. The RNA was treated with RNase-free DNase (Ambion, TX) to remove genomic DNA contamination. Total RNA was then reverse-transcribed to cDNA using the Super-Script II (Invitrogen), and the target genes were amplified using Syber Green Master Mix (Applied Biosystems, Foster City CA). The amplification was performed in real-time PCR system HT7900 (Applied Biosystems) using the following conditions: initial denaturation at  $95^\circ\text{C}$  for 2 min, followed by 35 cycles performed at  $95^\circ\text{C}$  for 30 s and  $60^\circ\text{C}$  for 30 s. The fold-induction/repression in gene expression by real-time RT-PCR was calculated after adjusting for actin using the formula  $2^{-\Delta\Delta Ct}$ . The primer sequences were reported previously (16,26) or described in Supplementary Table 1.

**Myocardial 4-hydroxynonenal, 3-nitrotyrosine accumulation, DNA fragmentation, caspase 3, and PARP activities.** 4-Hydroxynonenal (4-HNE), 3-nitrotyrosine (3-NT) (markers of oxidative/nitrative stress), DNA fragmentation, caspase 3, and PARP activities (markers of cell death) in LV tissue extracts/homogenates were determined using kits from Cell Biolabs (San Diego, CA); Hycult Biotechnology (Uden, the Netherlands); Roche Diagnostics (Indianapolis, IN); BioVision (Mountain View, CA); and Trevigen (Gaithersburg, MD), according to manufacturer's protocols as described (16,28).

**Myocardial AGE accumulation.** The AGE protein adducts were determined from LV tissue homogenates using an OxiSelect AGE enzyme-linked immunosorbent assay (ELISA) kit according to the manufacturer's instructions (Cell Biolabs).

**Western immunoblot analysis.** LV tissues were homogenized in mammalian tissue protein extraction reagent (TPER; Pierce Biotechnology, Rockford, IL) supplemented with protease and phosphatase inhibitors (Roche Diagnostics) and were lysed in radioimmunoprecipitation assay buffer supplemented with

protease and phosphate inhibitors. Then the samples were kept on ice for 1 h, followed by centrifugation at 13,000 rpm for 30 min at  $4^\circ\text{C}$ . The supernatants were carefully collected, and protein content was determined using a Lowry assay kit (Bio-Rad, Hercules, CA). A total of 30  $\mu\text{g}$  protein was resolved in 12% SDS-PAGE and transferred to nitrocellulose membranes (GE Healthcare). Blocking was done for 2 h at room temperature with 5% nonfat skimmed milk powder prepared in PBS containing 0.1% Tween 20 (Sigma). After washing with PBS with Tween 20, membranes were probed with mouse monoclonal inducible nitric oxide synthase (iNOS) antibody (Cell Signaling Technologies, Beverly, MA), anti-rabbit p38 MAPK, anti-rabbit phospho-p38 (Thr180/Tyr182) MAPK, or Jun NH<sub>2</sub>-terminal kinase (JNK) and phospho JNK (Thr183/Tyr185) used at a 1:1,000 dilution and incubated overnight at  $4^\circ\text{C}$ . The source of the antibody used for the detection of  $CB_1R$ s in the myocardial tissues were previously described (27). After subsequent washing with PBS with Tween 20, the secondary antibody, goat anti-rabbit horseradish peroxidase (Pierce Biotechnology), was used and incubated at room temperature for 1 h. The membranes then were developed using a chemiluminescence detection kit (SuperSignal West Pico substrate; Pierce Biotechnology). Blots were quantified using the Bio-Rad Quantity One program.

**Sirius Red staining for collagen.** LV myocardial sections were stained with Picrosirius Red satin solution for 1 h at room temperature. Then slides were washed in two changes of acidified water (0.5% acetic acid) for 2 min, and excess water was removed by blotting. Finally, the sections were dehydrated in 100% alcohol and cleared in xylene and mounted with cover glass (16). The quantification was performed as described at <http://rsbweb.nih.gov/ij/docs/examples/stained-sections/index.html>.

**Statistical analysis.** The results were expressed as mean  $\pm$  SEM. Differences among experimental groups were evaluated by ANOVA or Student *t* test if appropriate, and the significance of differences between groups was assessed by Tukey post hoc test. The analysis was performed using a statistical software package (GraphPad Prism 5; GraphPad Software, Inc., La Jolla, CA). Significance was defined as  $P < 0.05$ .

## RESULTS

**Metabolic variables.** Induction of diabetes by multiple doses of STZ led to reduction in the body weights with increase in the blood glucose levels in WT and  $CB_1^{+/+}$   $CB_1^{-/-}$  mice, respectively (Supplementary Figs. 1, 2A, and 2B). However, the blood glucose levels were not different during the course of the 12-week study period in  $CB_1^{-/-}$  and  $CB_1^{+/+}$  mice or in WT mice treated with vehicle or  $CB_1R$  antagonists SR141716 (SR1) and AM281 (AM) (Supplementary Figs. 1A and 2A). Similarly, there were no significant differences in the HbA<sub>1c</sub> levels (Supplementary Figs. 1C and 2C) and the pancreatic insulin content among corresponding groups (Supplementary Figs. 1D and 2D), respectively.

**Diabetes increases myocardial  $CB_1R$  expression and endocannabinoid anandamide levels: improved diabetes-induced cardiac dysfunction in  $CB_1^{-/-}$  mice.** Diabetic cardiomyopathy was associated with enhanced LV  $CB_1R$  expression and anandamide (also known as *N*-arachidonylethanolamide; AEA) levels compared with nondiabetic animals (control) (Fig. 1A and B; Supplementary Figs. 3 and 4).

Diabetic cardiomyopathy in  $CB_1^{+/+}$  mice was characterized by decreased load-dependent (+dP/dt; ejection fraction, stroke work, cardiac output) and load-independent ( $E_{\text{max}}$  dP/dt<sub>max</sub>–end-diastolic volume relation, preload-recruitable stroke work) indices of LV systolic contractile function, and impaired diastolic performance (decreased  $-dP/dt$ , prolonged time constants of LV pressure decay [ $\tau_{\text{Weiss}}$  and  $\tau_{\text{Giantz}}$ ], increased LV end-diastolic pressure, and decreased the slope of the end-diastolic pressure-volume relation [an index of LV stiffness]) (Fig. 1C and D). The diabetes-induced cardiac dysfunction was less pronounced in  $CB_1^{-/-}$  mice than in  $CB_1^{+/+}$  mice (Fig. 1C and D). There was no difference in the cardiac function in control  $CB_1^{-/-}$  and  $CB_1^{+/+}$  mice. The baseline heart rates were similar in both  $CB_1^{-/-}$  and  $CB_1^{+/+}$  mice ( $520 \pm 15$ ,  $n = 9$ , vs.  $529 \pm 19$ ,  $n = 9$ )

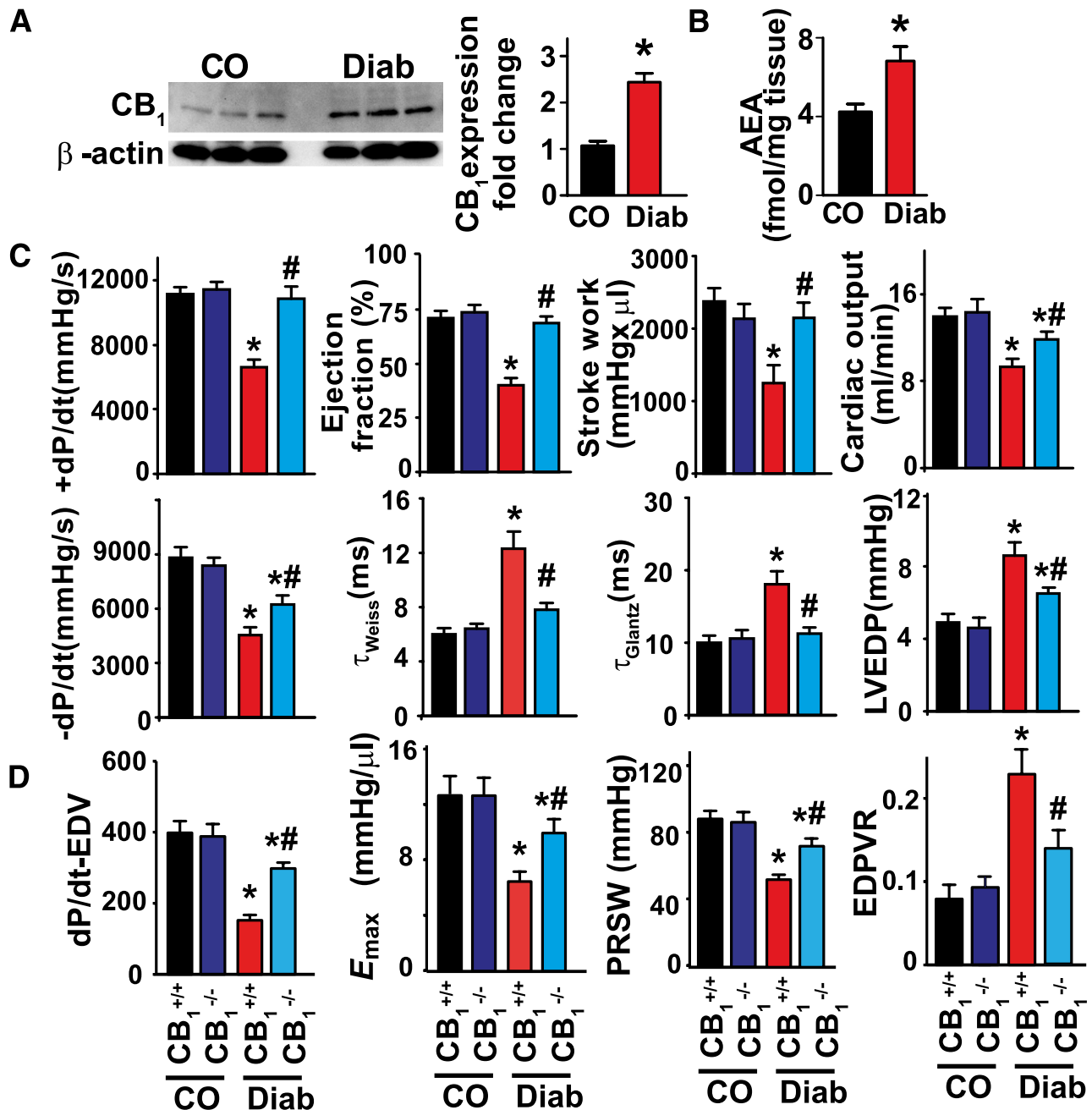


**FIG. 1.** Enhanced CB<sub>1</sub>R expression and endocannabinoid (AEA) levels in diabetic hearts; improved diabetes-induced cardiac dysfunction in CB<sub>1</sub><sup>-/-</sup> mice. **A:** After 12 weeks of established diabetes, mice were killed, heart left ventricles were excised, and protein samples were analyzed for CB<sub>1</sub>R expression by Western blot analysis. \**P* < 0.05 vs. control (CO). **B:** Levels of myocardial anandamide (AEA) were determined by liquid chromatography–mass spectrophotometry technique as described in RESEARCH DESIGN AND METHODS. \**P* < 0.05 vs. control. **C:** Twelve weeks of diabetes in CB<sub>1</sub><sup>+/+</sup> mice was characterized by decreased systolic (attenuated load-dependent [+dP/dt; ejection fraction, stroke work, cardiac output] and load-independent [D] [*E*<sub>max</sub>, dP/dt<sub>max</sub>-end-diastolic volume relation; preload-recruitable stroke work {PRSW}] indices of LV contractile function) and diastolic (decreased -dP/dt, prolonged time constants of LV pressure decay [τ<sub>Weiss</sub> and τ<sub>Glantz</sub>], increased LV end-diastolic pressure [LVEDP] [C], and decreased the slope of the end-diastolic pressure-volume relation [EDPVR; an index of LV stiffness [C, D]]) functions. The diabetes-induced cardiac dysfunction was less pronounced in CB<sub>1</sub><sup>-/-</sup> mice than in CB<sub>1</sub><sup>+/+</sup> mice (C and D). \**P* < 0.05 vs. CB<sub>1</sub><sup>+/+</sup> control (CO), #*P* < 0.05 vs. CB<sub>1</sub><sup>+/+</sup> diabetes (Diab); *n* = 6–9/group. (A high-quality color representation of this figure is available in the online issue.)

and were decreased to a similar extent after 3 months of diabetes (467 ± 21, *n* = 9, vs. 452 ± 20, *n* = 9), respectively. **Attenuated diabetes-induced myocardial inflammation, oxidative/nitrative stress, β-MHC isozyme switch, and AT<sub>1</sub>R expression in CB<sub>1</sub><sup>-/-</sup> mice.** LV mRNA expression of inflammatory cytokines, such as tumor necrosis factor (TNF)-α, interleukin (IL)-1β, adhesion molecules (intracellular adhesion molecule [ICAM]-1/vascular cell

adhesion molecule [VCAM]-1) (Fig. 2A), iNOS but not endothelial and neuronal nitric oxide synthases (eNOS and nNOS), cyclooxygenase 2 (COX2) (Fig. 2B; Supplementary Fig. 5), AT<sub>1</sub>R, and p47phox (Fig. 2D), was upregulated in the diabetic myocardium. This result was concordant with the profound oxidative/nitrative stress, characterized by the accumulation of lipid peroxidation product 4-hydroxynonenal and 3-NT (Fig. 2E), enhanced β-MHC isozyme switch

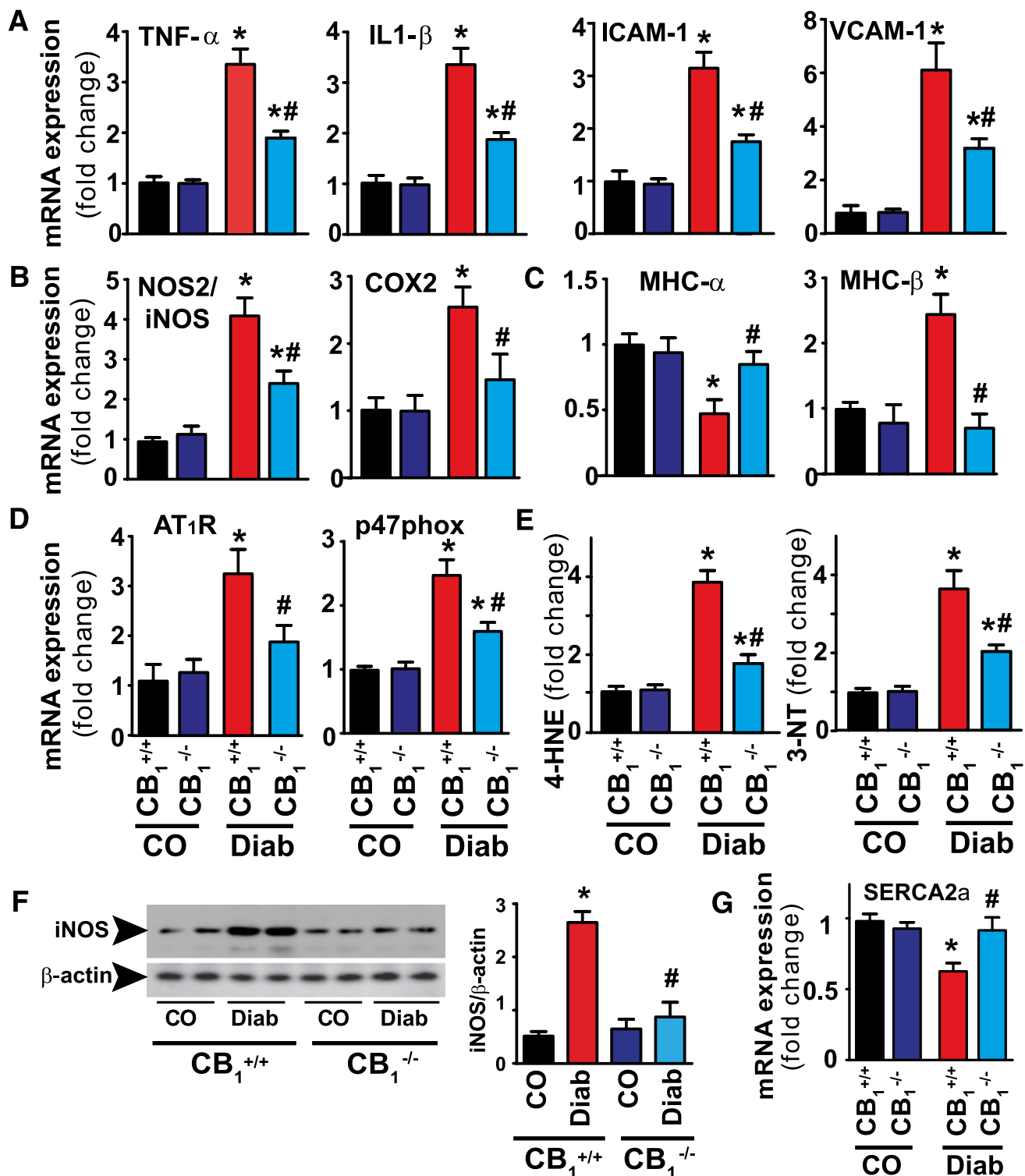


**FIG. 2.** Attenuation of diabetes-induced myocardial inflammation, oxidative/nitritive stress,  $\beta$ -MHC isozyme switch, and AT<sub>1</sub>R expression in CB<sub>1</sub><sup>-/-</sup> mice. **A:** LV mRNA expressions of inflammatory cytokines and adhesion molecules. **B:** iNOS and COX2. **C:**  $\alpha$ - and  $\beta$ -MHC. **D:** AT<sub>1</sub>R and p47phox NADPH isoform. **E:** Oxidative/nitritive stress was determined by measuring 4-HNE and 3-NT in the LV myocardial tissues. **F:** Protein of iNOS in the respective groups. **G:** SERCA2a. \* $P < 0.05$  vs. WT/CB<sub>1</sub><sup>+/+</sup> control (CO); # $P < 0.05$  vs. CB<sub>1</sub><sup>+/+</sup> diabetes (Diab);  $n = 8-9$ /group. (A high-quality color representation of this figure is available in the online issue.)

(decrease in  $\alpha$  and increase in  $\beta$  expression [Fig. 2C]), increased iNOS protein expression, and decreased SERCA2a mRNA expression (Fig. 2F and G). These deleterious effects induced by diabetes were ameliorated in mice lacking the CB<sub>1</sub>R.

**Attenuated diabetes-induced myocardial RAGE and AGE expression/accumulation, MAPK activation, and cell death in CB<sub>1</sub><sup>-/-</sup> mice.** Diabetes increased LV RAGE mRNA expression, AGE accumulation (Fig. 3A), p38/JNK MAPK induction (Fig. 3B), enhanced caspase 3, PARP

activation, and DNA fragmentation in CB<sub>1</sub><sup>+/+</sup> diabetic animals (Fig. 3C and D). These changes were attenuated in mice lacking the CB<sub>1</sub>R.

**Attenuated diabetes-induced myocardial fibrosis in CB<sub>1</sub><sup>-/-</sup> mice.** Diabetes induced marked LV interstitial fibrosis (Fig. 4A) and enhanced mRNA expressions of fibrotic markers (connective tissue growth factor, transforming growth factor-β, fibronectin, and collagen-I) (Fig. 4B) in the

CB<sub>1</sub><sup>+/+</sup> mice, which were blunted in diabetic CB<sub>1</sub><sup>-/-</sup> mice (Fig. 4A and B).

**CB<sub>1</sub>R inhibition attenuates diabetes-induced cardiac dysfunction.** Chronic treatment (11 weeks) with CB<sub>1</sub>R antagonist SR141716/rimonabant (SR1) improved both systolic and diastolic cardiac dysfunction associated with diabetes (Fig. 5A and B). Four weeks of treatment of 8-week diabetic mice with rimonabant also resulted in similar

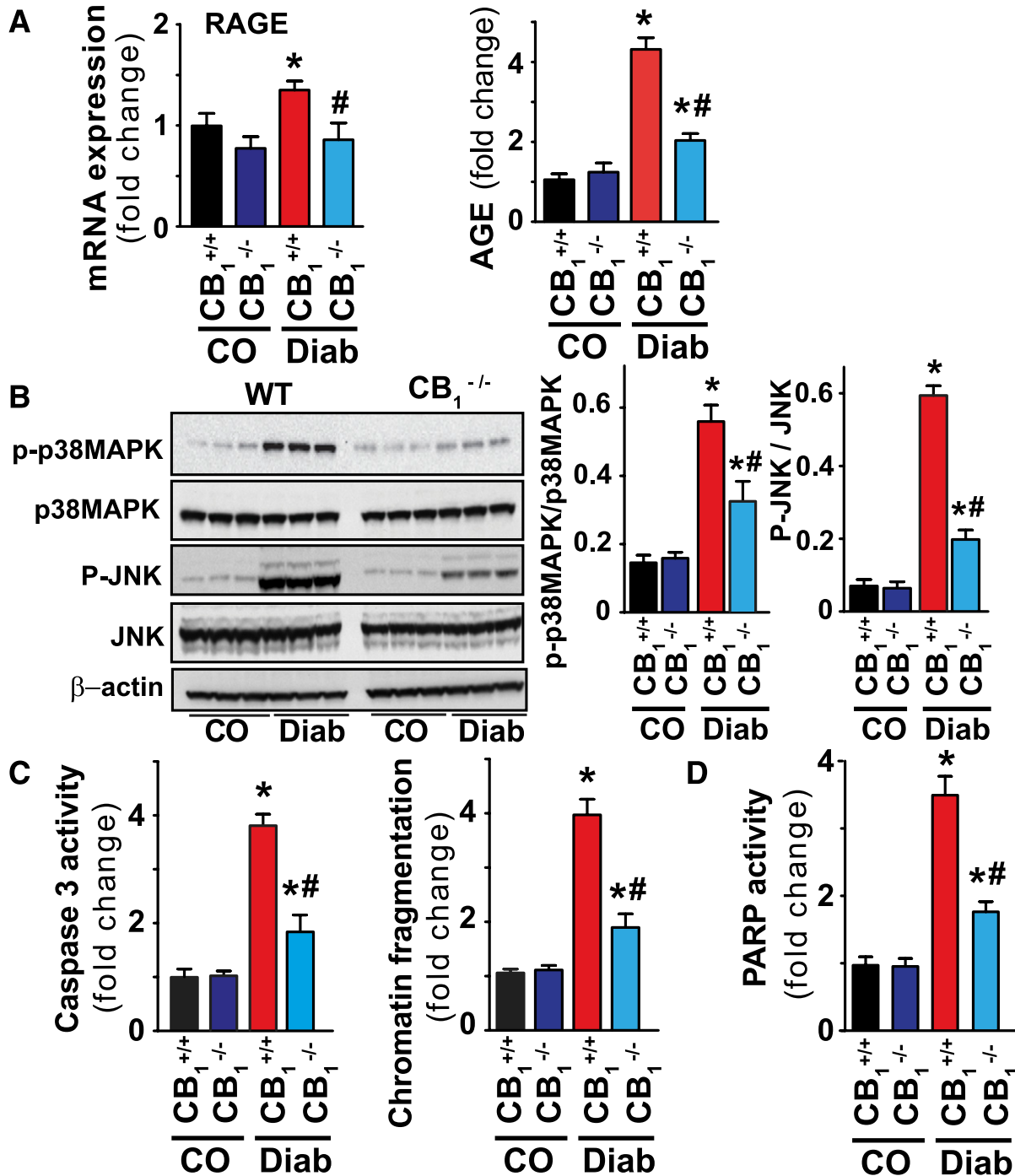


**FIG. 3.** Attenuated diabetes-induced myocardial RAGE and AGE expression/accumulation, MAPK activation, and cell death in CB<sub>1</sub><sup>-/-</sup> mice. **A:** LV mRNA expression of RAGE and accumulation of AGEs in the myocardium measured by ELISA. **B:** Representative Western immunoblot for the analysis of MAPKs (p38 and JNK) in the myocardial tissues. \**P* < 0.05 vs. CB<sub>1</sub><sup>+/+</sup> control (CO); #*P* < 0.05 vs. CB<sub>1</sub><sup>+/+</sup> diabetes (Diab); *n* = 6/group. **C** and **D:** Markers of cell death (PARP and caspase 3 activities and chromatin fragmentation) in the LV myocardial tissues from the respective groups. \**P* < 0.05 vs. WT/CB<sub>1</sub><sup>+/+</sup> control (CO); #*P* < 0.05 vs. CB<sub>1</sub><sup>+/+</sup> diabetes (Diab); *n* = 8/group. (A high-quality color representation of this figure is available in the online issue.)

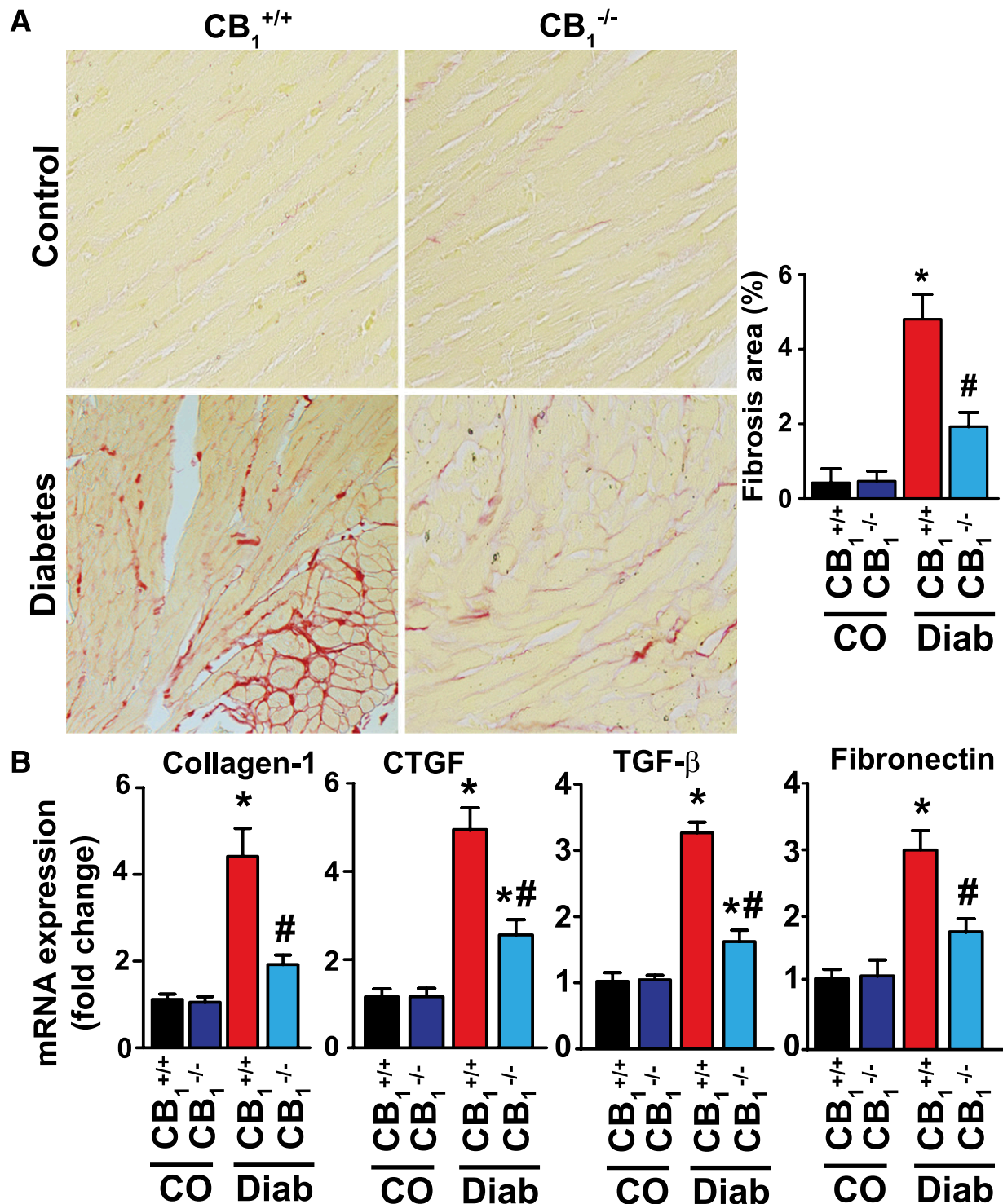


**FIG. 4.** Attenuation of diabetes-induced myocardial fibrosis in CB<sub>1</sub><sup>-/-</sup> mice. **A:** Representative formalin-fixed paraffin-embedded myocardial tissue sections stained with Sirius Red, indicating the marked interstitial fibrosis in the WT diabetic mice, which was attenuated in CB<sub>1</sub><sup>-/-</sup> mice. \**P* < 0.05 vs. CB<sub>1</sub><sup>+/+</sup> control (CO); #*P* < 0.05 vs. CB<sub>1</sub><sup>+/+</sup> diabetes (Diab); *n* = 6/group. **B:** mRNA expression of fibrosis markers in the myocardial tissues. \**P* < 0.05 vs. CB<sub>1</sub><sup>+/+</sup> control (CO); #*P* < 0.05 vs. CB<sub>1</sub><sup>+/+</sup> diabetes (Diab); *n* = 9/group. CTGF, connective tissue growth factor. (A high-quality digital representation of this figure is available in the online issue.)

but less pronounced LV functional improvements (Supplementary Fig. 6).

**CB<sub>1</sub>R inhibition attenuates diabetes-induced myocardial inflammation, oxidative/nitrative stress, β-MHC isozyme switch, AT<sub>1</sub>R, RAGE and AGE expression/accumulation, p38/JNK MAPK activation, and cell death.** Diabetes enhanced LV myocardial inflammation (Fig. 6A and B),

oxidative/nitrative stress (Fig. 6B, D, and G), mRNA expression of AT<sub>1</sub>R, p47phox (Fig. 2D), RAGE, accumulation of AGE (Fig. 2F), β-MHC isozyme switch (Fig. 2C), and decreased SERCA2 mRNA, which were attenuated by chronic treatment (11 weeks) of diabetic animals with CB<sub>1</sub>R antagonists SR141716/rimonabant (SR1) and AM281 (AM). Chronic treatment also attenuated the diabetes-induced LV

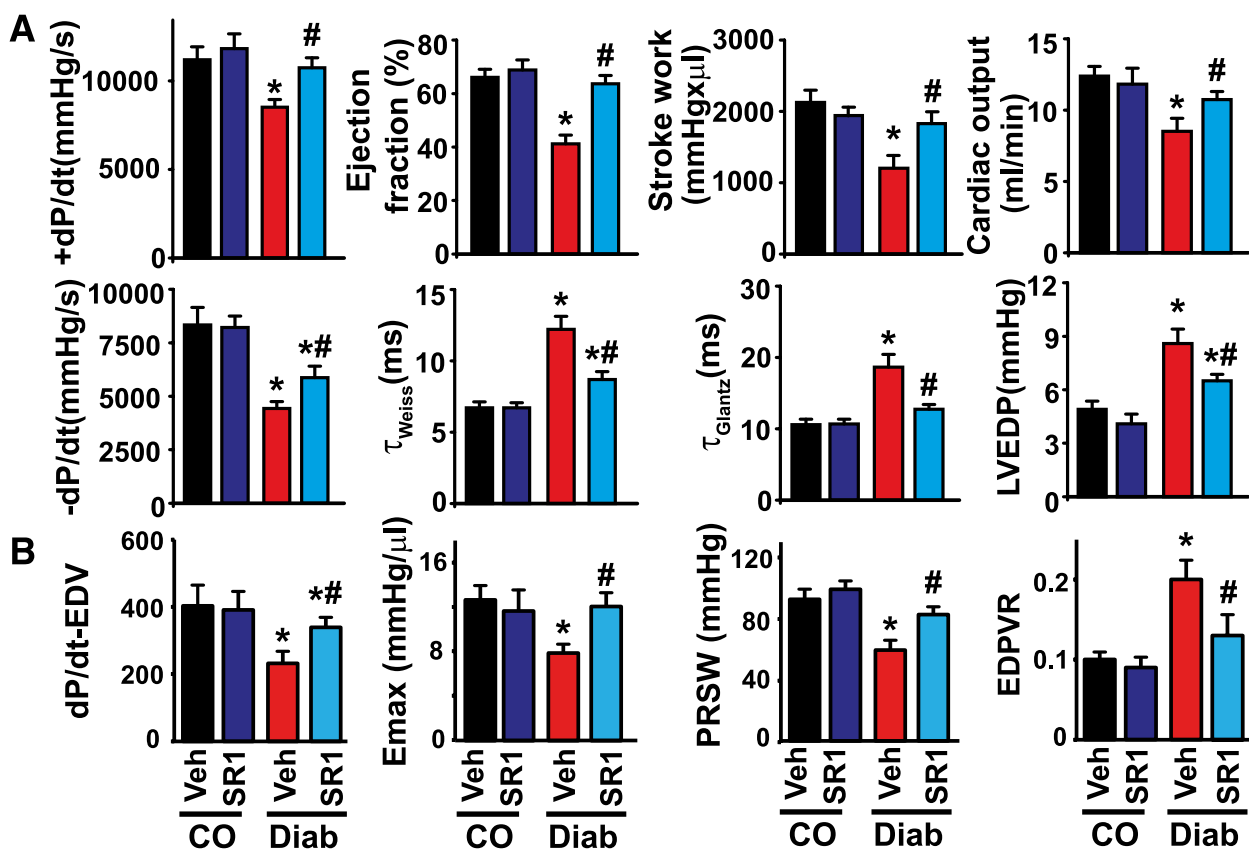


**FIG. 5.** Attenuation of diabetes-induced cardiac dysfunction by CB<sub>1</sub>R inhibition. **A:** Twelve weeks of diabetes in control (CO) mice was characterized by decreased systolic (attenuated load-dependent [ $+dP/dt$ ; ejection fraction, stroke work, cardiac output] and load-independent [ $-dP/dt$ ,  $dP/dt_{max}$ -end-diastolic volume relation; preload-recrutable stroke work (PRSW)] indices of LV contractile function) and diastolic (decreased  $-dP/dt$ , prolonged time constants of LV pressure decay [ $\tau_{Weiss}$  and  $\tau_{Glantz}$ ], increased LV end-diastolic pressure (LVEDP) (**B**), and decreased the slope of the end-diastolic pressure-volume relation (EDPVR; an index of LV stiffness [**B**]) functions. Eleven months of treatment with rimonabant (SR141716/SR1) attenuated the diabetes-induced cardiac dysfunction (**A** and **B**). \* $P < 0.05$  vs. vehicle/control (CO); # $P < 0.05$  vs. diabetes (Diab);  $n = 6-9$ /group. **B:** Representative pressure-volume loops after vena cava inferior occlusions demonstrate attenuation of the contractile function and increased diastolic stiffness in diabetic hearts, which is attenuated by CB<sub>1</sub>R blockade with SR1. Treatment of 8-week diabetic mice for 4 weeks with SR1 attenuated the diabetes-induced functional alterations (Supplementary Fig. 6). \* $P < 0.05$  vs. vehicle/control (CO); # $P < 0.05$  vs. diabetes (Diab);  $n = 5-7$ /group. (A high-quality color representation of this figure is available in the online issue.)

MAPK activation (Fig. 7A) and apoptotic and PARP-dependent cell death (Fig. 7B and C).

**CB<sub>1</sub>R inhibition attenuates diabetes-induced myocardial fibrosis.** Diabetes enhanced myocardial fibrosis characterized by increased collagen accumulation (Fig. 8A) and enhanced expression of mRNA markers of fibrosis (Fig. 8B), which were attenuated by chronic treatment (11 weeks) of diabetic animals with CB<sub>1</sub>R antagonists SR1 and AM.

## DISCUSSION

The salient findings emanating from the current study are as follows: 1) diabetes leads to upregulation of CB<sub>1</sub>R expression and increase in endocannabinoid anandamide/AEA levels in the myocardium; 2) diabetes-induced myocardial dysfunction is improved in CB<sub>1</sub><sup>-/-</sup> mice or in diabetic mice treated with CB<sub>1</sub> antagonist; 3) genetic deletion or pharmacological inhibition of CB<sub>1</sub>R attenuates MAPK activation, cell death, inflammation, and oxidative/nitrative stress in diabetic hearts; 4) likewise, it mitigates expression of RAGE, AT<sub>1</sub>R p47(phox) NADPH oxidase subunit, and impaired expression of SERCA2a and  $\beta$ -MHC isozyme switch; and 5) the diabetes-induced myocardial accumulation of AGEs and fibrosis are attenuated in CB<sub>1</sub><sup>-/-</sup> mice or in diabetic mice treated with CB<sub>1</sub> antagonists.

CB<sub>1</sub>R is expressed in endothelial (29,37,38), vascular smooth muscle (39,40), and inflammatory cells (30,31) and in cardiomyocytes (26,27,41). It is noteworthy that activation of cardiovascular CB<sub>1</sub>R by overproduced endocannabinoids has been implicated in the development of pathophysiological alterations and compromised cardiovascular function associated with various forms of shock, cirrhotic cardiomyopathy, and heart failure (21,26-28). There is also increasing recognition that in various pathological conditions, CB<sub>1</sub>R activation by endocannabinoids may trigger activation of signaling pathways (e.g., p38 and JNK-MAPKs promoting cell death) (21,27,42,43). Recent studies have also demonstrated that CB<sub>1</sub>R activation by endocannabinoids or synthetic agonists in human coronary artery endothelial cells (29) and in primary human or murine cardiomyocytes (27) triggered increased p38 and JNK activation and ROS generation promoting cell death. CB<sub>1</sub>R activation also induced ROS generation and TNF- $\alpha$  production in human macrophages that depended on the p38 MAPK pathway and could be attenuated by its inhibition (30). p38 MAPK inhibition also attenuated CB<sub>1</sub>-mediated cell death in endothelial cells and cardiomyocytes (27,29). Consistently with the above-mentioned studies in preclinical models of heart failure (26-28), atherosclerosis (31,44), and diabetic retinopathy (34),

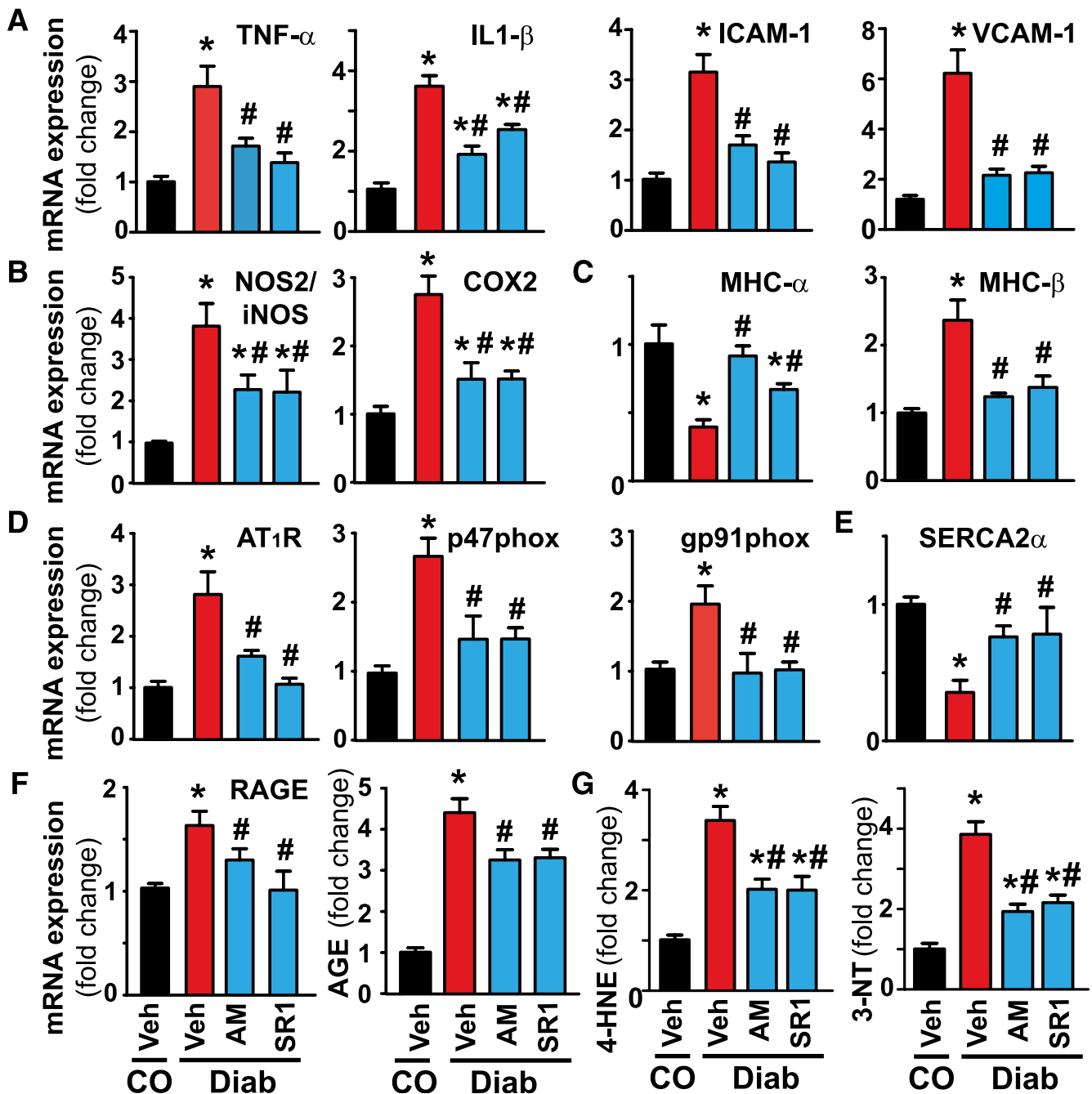


**FIG. 6.** Attenuation of diabetes-induced myocardial inflammation, oxidative/nitrate stress,  $\beta$ -MHC isozyme switch, and AT<sub>1</sub>R expression by CB<sub>1</sub>R antagonists. **A:** LV mRNA expressions of inflammatory cytokines and adhesion molecules. **B:** iNOS and COX2. **C:**  $\alpha$ - and  $\beta$ -MHC. **D:** AT<sub>1</sub>R, p47phox, gp91phox, and NADPH isoforms. **E:** SERCA2 $\alpha$ . **F:** mRNA expression of RAGE and accumulation of AGE in the myocardium measured by ELISA. **G:** Oxidative/nitrate stress determined by measuring 4-HNE and 3-NT in the LV myocardial tissues in the respective groups as indicated. \* $P < 0.05$  vs. vehicle control (CO); # $P < 0.05$  vs. diabetes (Diab),  $n = 8$ –9/group. AM/SR1 treatments alone in control mice had no significant effect on any of the markers studied (not shown) compared with vehicle-treated controls (CO). (A high-quality color representation of this figure is available in the online issue.)

CB<sub>1</sub> deletion or pharmacological inhibition limits the vascular or myocardial inflammation and/or oxidative/nitrate stress and interrelated cell death and disease progression. CB<sub>1</sub> antagonists also exerted numerous unexpected beneficial effects (e.g., anti-inflammatory effects) in clinical trials of obesity beyond their effects on body weight (23,25,35,45), and peripheral CB<sub>1</sub>R blockade appears to be a promising approach in the treatment of visceral obesity and its cardiometabolic complications (45,46).

It is noteworthy that increased plasma endocannabinoid levels positively correlate with coronary circulatory dysfunction in human obesity (32). We found increased CB<sub>1</sub>R expression and endocannabinoid anandamide levels in the left ventricle of diabetic hearts, which is consistent with elevated anandamide levels reported in the retina of patients with diabetic retinopathy (47). Increased endocannabinoid levels have also been reported in serum of patients with type 2 diabetes and their subcutaneous tissue (35). Although the mechanism of marked upregulation of

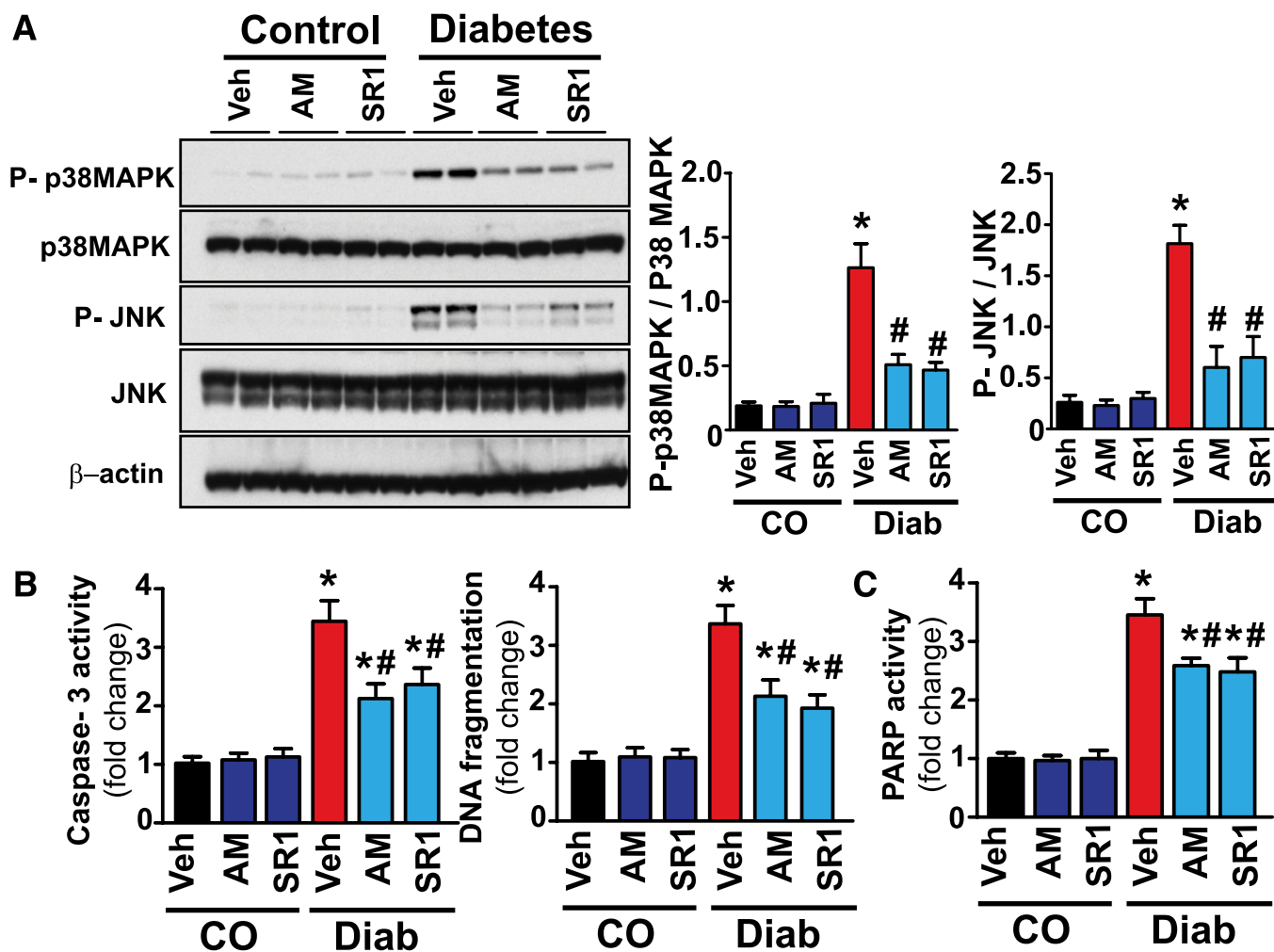


**FIG. 7.** Attenuation of diabetes-induced myocardial MAPK activation and apoptosis by CB<sub>1</sub>R antagonists. **A:** Representative immunoblot for the p38/JNK MAPKs in the myocardial tissues from the respective groups. \* $P < 0.05$  vs. vehicle/AM/SR1 control (CO); # $P < 0.05$  vs. diabetes (Diab),  $n = 6$ /group. **B** and **C:** Cell death markers in the respective groups as indicated. \* $P < 0.05$  vs. vehicle/AM/SR1 control (CO); # $P < 0.05$  vs. diabetes (Diab),  $n = 8$ /group. (A high-quality color representation of this figure is available in the online issue.)

CB<sub>1</sub>Rs in various peripheral tissues during multiple disease conditions associated with increased inflammation and/or oxidative stress has not been evaluated in much detail (21,45), this process most likely may involve activation of ROS- and/or inflammation-dependent transcription factors. Indeed, in rat mesangial cells, high glucose upregulates CB<sub>1</sub> mRNA expression in an NF- $\kappa$ B-dependent manner. Similarly, hyperglycemia-induced upregulation of CB<sub>1</sub> has also been reported in retina pigment epithelial cells recently (rev. in 35). CB<sub>1</sub> antagonists attenuated the high glucose-induced apoptosis in mesangial, retina pigment epithelial, and endothelial cells (35). Reactive oxygen and nitrogen species and inflammatory mediators such as TNF- $\alpha$ , which are also known to be triggered/upregulated by hyperglycemia, have been implicated in enhanced endocannabinoid production through the activation of NF- $\kappa$ B and other pathways in several cell types (including monocytes/macrophages and cardiomyocytes), as well as by inactivation and/or downregulation of the endocannabinoid-metabolizing enzyme fatty acid amide hydrolase. Consistently, hyperglycemia induced fatty acid amide hydrolase- and CB<sub>1</sub>-dependent cell death in retina pigment epithelial cells (rev. in 35). Notably, fatty acid amide hydrolase knockout mice, which have approximately two- to threefold increased

myocardial anandamide levels, have markedly increased mortality, cardiac dysfunction, and myocardial cell death in acute and chronic heart failure models, which are attenuated by CB<sub>1</sub> antagonists (28). More importantly, elevated plasma endocannabinoid levels show very strong positive correlation with coronary circulatory dysfunction and adverse cardiac events in obese human subjects (32).

Growing evidence implies that oxidative/nitrative stress together with activation of various proinflammatory and cell death pathways play pivotal roles in the development of complex biochemical, mechanical, and structural alterations associated with diabetic cardiomyopathy (3–6,10,14–16). Unfortunately, despite the accumulating knowledge obtained during the past decades, the treatment of diabetic cardiomyopathy is poor and largely symptomatic (1).

In the current study, using a well-characterized mouse model of type 1 diabetic cardiomyopathy (3,5,14,16), we evaluated the effects of genetic deletion or pharmacological inhibition of CB<sub>1</sub>Rs with selective CB<sub>1</sub> antagonists (for 11 weeks administered after the destruction of pancreatic  $\beta$ -cells and development of frank type 1 diabetes) on myocardial dysfunction, inflammation, oxidative/nitrative stress, cell death, fibrosis, and interrelated signaling pathways.

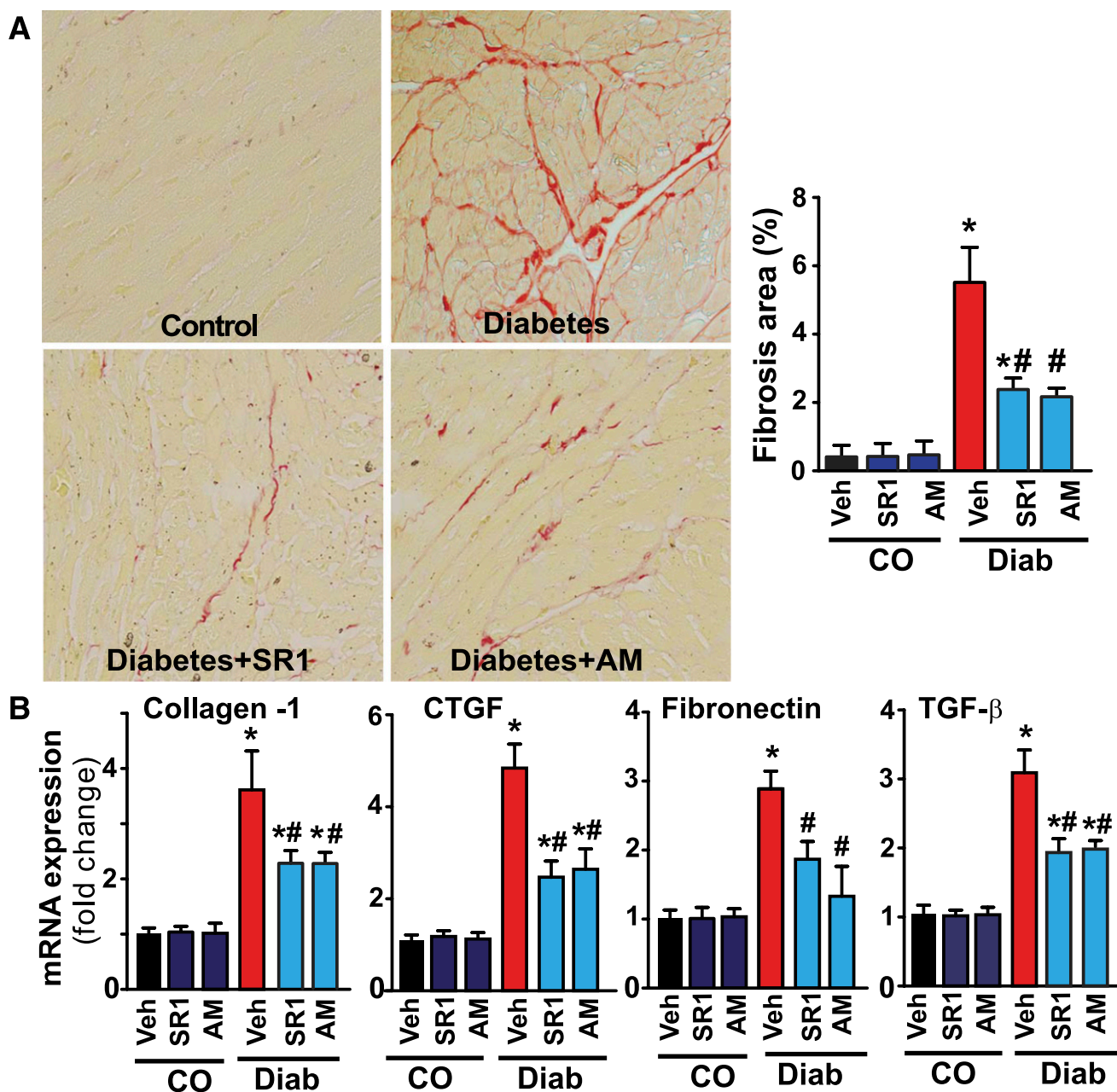


**FIG. 8.** Attenuation of diabetes-induced myocardial fibrosis by CB<sub>1</sub>R antagonists. **A:** The representative formalin-fixed paraffin-embedded myocardial tissue sections stained with Sirius Red, indicating the marked fibrosis in the diabetic mice, which was attenuated by CB<sub>1</sub>R antagonists. \**P* < 0.05 vs. vehicle/AM/SR1 control (CO); #*P* < 0.05 vs. diabetes (Diab), *n* = 6/group. **B:** mRNA expression of fibrosis markers in the myocardial tissues. \**P* < 0.05 vs. vehicle/AM/SR1 control (CO); #*P* < 0.05 vs. diabetes (Diab), *n* = 9/group. (A high-quality digital representation of this figure is available in the online issue.)

We also evaluated the effect of CB<sub>1</sub> inhibition on cardiac dysfunction associated with already-established diabetic cardiomyopathy (4 weeks' treatment of 8-week diabetic mice).

Consistent with previous reports (3,5–7,13–16), diabetic cardiomyopathy was characterized by declined diastolic and systolic myocardial performance, increased oxidative/nitrative stress (4-HNE, 3-NT, iNOS), activation of various stress signaling pathways (e.g., JNK and p38 MAPK), enhanced expression of RAGE and AT<sub>1</sub>R, p47(phox) NADPH oxidase subunit, accumulation of AGEs, inflammation (increased expression of TNF-α, IL-1β, COX2, adhesion molecules ICAM-1 and VCAM-1), β-MHC isozyme switch, myocardial fibrosis, and decreased expression of SERCA2a.

Compelling evidence (both from rodent models of STZ-induced type 1 diabetes and human myocardial biopsies) suggests that the renin-angiotensin system is upregulated with diabetes and angiotensin II locally through AT<sub>1</sub>R and is overexpressed in diabetic hearts or in cardiomyocytes exposed to high glucose, contributing to the development of diabetic cardiomyopathy (3,10–13). The beneficial effects of AT<sub>1</sub>R blockade in diabetic hearts involve, but are not limited to, the attenuation of myocardial NADPH oxidase-dependent (such as p47phox) ROS generation, inflammation, cell death, fibrosis, and contractile dysfunction (3,10–13). Xanthine oxidase, cyclooxygenase, mitochondrial electron transport chain, activated inflammatory cells, and uncoupled endothelial nitric oxide synthase may also

represent additional sources of ROS generation in diabetic hearts (4). Convincing *in vitro*, *ex vivo*, and *in vivo* evidence suggests that high glucose-induced increased iNOS expression contributes to cardiac dysfunction associated with type 1 diabetic cardiomyopathy via formation of reactive nitrogen species such as peroxynitrite through the rapid diffusion-limited reaction of superoxide anion (derived from NADPH oxidase and other sources) and nitric oxide derived from iNOS (rev. in 4). The above-mentioned reaction is faster than the decomposition of the superoxide by superoxide dismutase; therefore, it results in loss of the beneficial effects of nitric oxide (it is immediately converted to reactive nitrogen species in the presence of superoxide before is able to exert its known protective effects) (4). High glucose-induced ROS/reactive nitrogen species also induces modifications of important proteins involved in Ca<sup>2+</sup> handling and myocardial contractility (e.g., SERCA2a) (4) and decrease of their expression/function (18–20), lipid peroxidation, oxidative DNA damage, activation of stress signaling, and other cell death pathways, among others (4). p38 MAPK activation appears to play an important role in pathogenesis of diabetic cardiomyopathy, since its pharmacological inhibition attenuates not only myocardial dysfunction, but also the expression of cardiac inflammatory markers, such as TNF- $\alpha$ , IL-1 $\beta$ , IL-6, and myocardial fibrosis (15).

Hyperglycemia and/or hyperglycemia-induced ROS (also involving enhanced AT<sub>1</sub>R expression/signaling) may lead to increased accumulation of products of nonenzymatic glycation/oxidation of proteins/lipids (AGE) and enhanced expression of their receptor (RAGE) in the vasculature and myocardium; these products are thought to play a key role in the development and progression of cardiovascular complications of diabetes (7,8). In hearts of type 1 diabetic rodents, increased expression of RAGE and accumulation of AGEs have been associated with diabetes-induced dysfunction and structural alterations (7,8). In diabetic heart failure patients with reduced LV ejection fraction, the fibrosis and accumulation of AGEs contribute to the increased diastolic stiffness, but in patients with normal LV ejection fraction, the increased cardiomyocyte resting tension is responsible for this phenomenon (9).

Genetic deletion of CB<sub>1</sub>R or its pharmacological inhibition with selective CB<sub>1</sub> antagonists attenuated the diabetes-induced myocardial dysfunction, expression of AT<sub>1</sub>R and RAGE, accumulation of AGEs, oxidative/nitrative stress and inflammation [4-HNE, 3-NT, iNOS, p47(phox), TNF- $\alpha$ , IL-1 $\beta$ , COX2, ICAM-1, and VCAM-1], activation of myocardial p38/JNK MAPKs, cell death, and fibrosis and also restored the impaired expression of SERCA2a and MHC isozyme switch.

Interestingly, in recent provocative studies, Hunyady's group (rev. in 48) proposed a paracrine transactivation of the CB<sub>1</sub> cannabinoid receptor by AT<sub>1</sub> and other G<sub>q</sub>/11 protein-coupled receptors, implying that this signaling may overlap in a pathological situation. Indeed, a recent study demonstrated that CB<sub>1</sub>R and AT<sub>1</sub>R functionally interact forming heteromers, resulting in the potentiation of AT<sub>1</sub>R signaling (49). AT<sub>1</sub>R-CB<sub>1</sub>R heteromers and enhancement of angiotensin II-mediated signaling were demonstrated in hepatic stellate cells from ethanol-administered rats (in which CB<sub>1</sub>R was upregulated), and CB<sub>1</sub> inhibition prevented the angiotensin II-mediated mitogenic signaling and profibrogenic gene expression (49) underlying the functional significance of this interaction. A recent study also described that chronic CB<sub>1</sub>R inhibition led to decreased vascular AT<sub>1</sub>R expression, NADPH

oxidase-derived vascular oxidative stress, and improved endothelial function in apolipoprotein E-deficient mice fed a cholesterol-rich diet (40). In cultured vascular smooth muscle cells, CB<sub>1</sub> antagonists reduced angiotensin II-mediated NADPH oxidase-dependent ROS generation and downregulated AT<sub>1</sub>R expression, whereas CB<sub>1</sub>R agonist upregulated AT<sub>1</sub>R, indicating that AT<sub>1</sub>R expression is directly regulated by the CB<sub>1</sub>R. In light of the above-mentioned observations, our current study demonstrating decreased AT<sub>1</sub>R and p47(phox) expression in hearts of CB<sub>1</sub> knockout diabetic mice or mice treated with CB<sub>1</sub> antagonists also suggests an important interaction of CB<sub>1</sub> and AT<sub>1</sub>R signaling. The downregulation of the AT<sub>1</sub>R-NADPH oxidase-ROS pathway by CB<sub>1</sub>R inhibition/genetic deletion could also contribute to decreased oxidative stress, AGE/RAGE accumulation/signaling, MAPK activation, cell death, and fibrosis observed under these conditions, in addition to the direct inhibitory effect of the overproduced endocannabinoid-CB<sub>1</sub> signaling on MAPK activation and its multiple above-discussed consequences in cardiovascular cell types. The attenuated myocardial fibrosis and AGE accumulation in hearts of the diabetic CB<sub>1</sub>R knockout mice or mice treated with SR141716/rimonabant is most likely responsible for the decreased diastolic stiffness observed.

It is noteworthy that our results also suggest that CB<sub>1</sub> inhibition may preserve its beneficial effects on contractile dysfunction even if administered after the development of established cardiomyopathy. This result coupled with recent studies demonstrating that CB<sub>1</sub>R blockade and/or its genetic deletion attenuates proteinuria and/or vascular inflammation and cell death in experimental models of type 1 diabetic nephropathy (33), retinopathy (34), and neuropathy (35), and increases pancreatic  $\beta$ -cell proliferation and mass before the complete destruction of these cells in early diabetes (50), are very exciting from a therapeutic point of view.

Collectively, our results strongly suggest that overactivation of endocannabinoid system and CB<sub>1</sub>Rs may play an important role in the pathogenesis of diabetic cardiomyopathy by facilitating AT<sub>1</sub>R expression/signaling, RAGE and AGE expression/accumulation/signaling, MAPK activation, oxidative/nitrative stress, inflammation, cell death, fibrosis, and contractile dysfunction. Conversely, CB<sub>1</sub>R inhibition may be of significant benefit in the treatment of diabetic cardiovascular complications and possibly other complications.

#### ACKNOWLEDGMENTS

This study was supported by the Intramural Research Program of NIH/NIAAA (to P.P.). B.H. was supported by an National Office for Research and Technology-Hungarian Scientific Research Fund-European Union 7th Framework fellowship (MB08-A80238). S.B. was supported by the Alexander von Humboldt Foundation and the European Commission (FP7-CIG-294278).

No potential conflicts of interest relevant to this article were reported.

M.R. researched data and reviewed, edited, and wrote the manuscript. S.B., M.K., P.M., W.-S.L., B.H., E.H., R.C., L.L., and G.H. researched data and contributed to discussion. K.M. contributed new reagents, edited the manuscript, and contributed to discussion. P.P. wrote the manuscript, reviewed and edited the manuscript, and contributed to discussion. P.P. is the guarantor of this work and, as such, had full access to all the data in the study and takes responsibility for the integrity of the data and the accuracy of the data analysis.

The authors are indebted to Judith Harvey-White (NIH/NIAAA) and Dr. George Kunos (NIH/NIAAA) for endocannabinoid measurements and Dr. Kunos for providing support and resources for the completion of this study.

## REFERENCES

- Fein FS. Diabetic cardiomyopathy. *Diabetes Care* 1990;13:1169–1179
- Regan TJ, Ahmed S, Haider B, Moschos C, Weisse A. Diabetic cardiomyopathy: experimental and clinical observations. *N J Med* 1994;91:776–778
- Kajstura J, Fiordaliso F, Andreoli AM, et al. IGF-1 overexpression inhibits the development of diabetic cardiomyopathy and angiotensin II-mediated oxidative stress. *Diabetes* 2001;50:1414–1424
- Pacher P, Beckman JS, Liaudet L. Nitric oxide and peroxynitrite in health and disease. *Physiol Rev* 2007;87:315–424
- Cai L, Wang Y, Zhou G, et al. Attenuation by metallothionein of early cardiac cell death via suppression of mitochondrial oxidative stress results in a prevention of diabetic cardiomyopathy. *J Am Coll Cardiol* 2006;48:1688–1697
- Wang Y, Feng W, Xue W, et al. Inactivation of GSK-3 $\beta$  by metallothionein prevents diabetes-related changes in cardiac energy metabolism, inflammation, nitrosative damage, and remodeling. *Diabetes* 2009;58:1391–1402
- Candido R, Forbes JM, Thomas MC, et al. A breaker of advanced glycation end products attenuates diabetes-induced myocardial structural changes. *Circ Res* 2003;92:785–792
- Bidasee KR, Zhang Y, Shao CH, et al. Diabetes increases formation of advanced glycation end products on Sarco(endo)plasmic reticulum Ca<sup>2+</sup>-ATPase. *Diabetes* 2004;53:463–473
- van Heerebeek L, Hamdani N, Handoko ML, et al. Diastolic stiffness of the failing diabetic heart: importance of fibrosis, advanced glycation end products, and myocyte resting tension. *Circulation* 2008;117:43–51
- Frustaci A, Kajstura J, Chimenti C, et al. Myocardial cell death in human diabetes. *Circ Res* 2000;87:1123–1132
- Raimondi L, De Paoli P, Mannucci E, et al. Restoration of cardiomyocyte functional properties by angiotensin II receptor blockade in diabetic rats. *Diabetes* 2004;53:1927–1933
- Privratsky JR, Wold LE, Sowers JR, Quinn MT, Ren J. AT1 blockade prevents glucose-induced cardiac dysfunction in ventricular myocytes: role of the AT1 receptor and NADPH oxidase. *Hypertension* 2003;42:206–212
- Westermann D, Rutschow S, Jäger S, et al. Contributions of inflammation and cardiac matrix metalloproteinase activity to cardiac failure in diabetic cardiomyopathy: the role of angiotensin type 1 receptor antagonism. *Diabetes* 2007;56:641–646
- Pacher P, Liaudet L, Soriano FG, Mabley JG, Szabó E, Szabó C. The role of poly(ADP-ribose) polymerase activation in the development of myocardial and endothelial dysfunction in diabetes. *Diabetes* 2002;51:514–521
- Westermann D, Rutschow S, Van Linthout S, et al. Inhibition of p38 mitogen-activated protein kinase attenuates left ventricular dysfunction by mediating pro-inflammatory cardiac cytokine levels in a mouse model of diabetes mellitus. *Diabetologia* 2006;49:2507–2513
- Rajesh M, Mukhopadhyay P, Bátkai S, et al. Cannabidiol attenuates cardiac dysfunction, oxidative stress, fibrosis, and inflammatory and cell death signaling pathways in diabetic cardiomyopathy. *J Am Coll Cardiol* 2010;56:2115–2125
- Dillmann WH. Diabetes mellitus induces changes in cardiac myosin of the rat. *Diabetes* 1980;29:579–582
- Malhotra A, Penpargkul S, Fein FS, Sonnenblick EH, Scheuer J. The effect of streptozotocin-induced diabetes in rats on cardiac contractile proteins. *Circ Res* 1981;49:1243–1250
- Dillmann WH. Diabetes and thyroid-hormone-induced changes in cardiac function and their molecular basis. *Annu Rev Med* 1989;40:373–394
- Dhalla NS, Liu X, Panagia V, Takeda N. Subcellular remodeling and heart dysfunction in chronic diabetes. *Cardiovasc Res* 1998;40:239–247
- Pacher P, Bátkai S, Kunos G. The endocannabinoid system as an emerging target of pharmacotherapy. *Pharmacol Rev* 2006;58:389–462
- Engeli S. Dysregulation of the endocannabinoid system in obesity. *J Neuroendocrinol* 2008;20(Suppl. 1):110–115
- Di Marzo V. The endocannabinoid system in obesity and type 2 diabetes. *Diabetologia* 2008;51:1356–1367
- Engeli S, Böhnke J, Feldpausch M, et al. Activation of the peripheral endocannabinoid system in human obesity. *Diabetes* 2005;54:2838–2843
- Silvestri C, Ligresti A, Di Marzo V. Peripheral effects of the endocannabinoid system in energy homeostasis: adipose tissue, liver and skeletal muscle. *Rev Endocr Metab Disord* 2011;12:153–162
- Mukhopadhyay P, Bátkai S, Rajesh M, et al. Pharmacological inhibition of CB1 cannabinoid receptor protects against doxorubicin-induced cardiotoxicity. *J Am Coll Cardiol* 2007;50:528–536
- Mukhopadhyay P, Rajesh M, Bátkai S, et al. CB1 cannabinoid receptors promote oxidative stress and cell death in murine models of doxorubicin-induced cardiomyopathy and in human cardiomyocytes. *Cardiovasc Res* 2010;85:773–784
- Mukhopadhyay P, Horváth B, Rajesh M, et al. Fatty acid amide hydrolase is a key regulator of endocannabinoid-induced myocardial tissue injury. *Free Radic Biol Med* 2011;50:179–195
- Rajesh M, Mukhopadhyay P, Haskó G, Liaudet L, Mackie K, Pacher P. Cannabinoid-1 receptor activation induces reactive oxygen species-dependent and -independent mitogen-activated protein kinase activation and cell death in human coronary artery endothelial cells. *Br J Pharmacol* 2010;160:688–700
- Han KH, Lim S, Ryu J, et al. CB1 and CB2 cannabinoid receptors differentially regulate the production of reactive oxygen species by macrophages. *Cardiovasc Res* 2009;84:378–386
- Sugamura K, Sugiyama S, Nozaki T, et al. Activated endocannabinoid system in coronary artery disease and antiinflammatory effects of cannabinoid 1 receptor blockade on macrophages. *Circulation* 2009;119:28–36
- Quercioli A, Pataky Z, Vincenti G, et al. Elevated endocannabinoid plasma levels are associated with coronary circulatory dysfunction in obesity. *Eur Heart J* 2011;32:1369–1378
- Barutta F, Corbelli A, Mastrocola R, et al. Cannabinoid receptor 1 blockade ameliorates albuminuria in experimental diabetic nephropathy. *Diabetes* 2010;59:1046–1054
- El-Remessy AB, Rajesh M, Mukhopadhyay P, et al. Cannabinoid 1 receptor activation contributes to vascular inflammation and cell death in a mouse model of diabetic retinopathy and a human retinal cell line. *Diabetologia* 2011;54:1567–1578
- Horváth B, Mukhopadhyay P, Haskó G, Pacher P. The endocannabinoid system and plant-derived cannabinoids in diabetes and diabetic complications. *Am J Pathol* 2012;180:432–442
- Pacher P, Nagayama T, Mukhopadhyay P, Bátkai S, Kass DA. Measurement of cardiac function using pressure-volume conductance catheter technique in mice and rats. *Nat Protoc* 2008;3:1422–1434
- Liu J, Gao B, Mirshahi F, et al. Functional CB1 cannabinoid receptors in human vascular endothelial cells. *Biochem J* 2000;346:835–840
- Rajesh M, Mukhopadhyay P, Bátkai S, et al. CB2-receptor stimulation attenuates TNF- $\alpha$ -induced human endothelial cell activation, trans-endothelial migration of monocytes, and monocyte-endothelial adhesion. *Am J Physiol Heart Circ Physiol* 2007;293:H2210–H2218
- Rajesh M, Mukhopadhyay P, Haskó G, Pacher P. Cannabinoid CB1 receptor inhibition decreases vascular smooth muscle migration and proliferation. *Biochem Biophys Res Commun* 2008;377:1248–1252
- Tiyerili V, Zimmer S, Jung S, et al. CB1 receptor inhibition leads to decreased vascular AT1 receptor expression, inhibition of oxidative stress and improved endothelial function. *Basic Res Cardiol* 2010;105:465–477
- Mach F, Montecucco F, Steffens S. Cannabinoid receptors in acute and chronic complications of atherosclerosis. *Br J Pharmacol* 2008;153:290–298
- Di Marzo V. Targeting the endocannabinoid system: to enhance or reduce? *Nat Rev Drug Discov* 2008;7:438–455
- Mukhopadhyay P, Pan H, Rajesh M, et al. CB1 cannabinoid receptors promote oxidative/nitrosative stress, inflammation and cell death in a murine nephropathy model. *Br J Pharmacol* 2010;160:657–668
- Dol-Gleizes F, Paumelle R, Visentin V, et al. Rimonabant, a selective cannabinoid CB1 receptor antagonist, inhibits atherosclerosis in LDL receptor-deficient mice. *Arterioscler Thromb Vasc Biol* 2009;29:12–18
- Kunos G, Tam J. The case for peripheral CB1 receptor blockade in the treatment of visceral obesity and its cardiometabolic complications. *Br J Pharmacol* 2011;163:1423–1431
- Tam J, Vemuri VK, Liu J, et al. Peripheral CB1 cannabinoid receptor blockade improves cardiometabolic risk in mouse models of obesity. *J Clin Invest* 2010;120:2953–2966
- Matias I, Wang JW, Moriello AS, Nieves A, Woodward DF, Di Marzo V. Changes in endocannabinoid and palmitoylethanolamide levels in eye tissues of patients with diabetic retinopathy and age-related macular degeneration. *Prostaglandins Leukot Essent Fatty Acids* 2006;75:413–418
- Gyombolai P, Pap D, Turu G, Catt KJ, Bagdy G, Hunyady L. Regulation of endocannabinoid release by G proteins: A paracrine mechanism of G protein-coupled receptor action. *Mol Cell Endocrinol*. 2 November 2011 [Epub ahead of print]
- Rozenfeld R, Gupta A, Gagnidze K, et al. AT1R-CB1R heteromerization reveals a new mechanism for the pathogenic properties of angiotensin II. *EMBO J* 2011;30:2350–2363
- Kim W, Doyle ME, Liu Z, et al. Cannabinoids inhibit insulin receptor signaling in pancreatic  $\beta$ -cells. *Diabetes* 2011;60:1198–1209